

Succinate dehydrogenase deficiency-driven succinate accumulation induces drug resistance in acute myeloid leukemia via ubiquitin-cullin regulation

Received: 7 November 2023

Accepted: 9 October 2024

Published online: 13 November 2024



Yifan Chen^{1,5}, Miao Xian^{1,5}, Wenwen Ying¹, Jiayi Liu¹, Shaowei Bing¹, Xiaomin Wang¹, Jiayi Yu¹, Xiaojun Xu², Senfeng Xiang¹, Xuejing Shao¹, Ji Cao^{1,3,4}, Qiaojun He^{1,3,4}, Bo Yang^{1,3,4} & Meidan Ying^{1,2,3,4}✉

Drug resistance is vital for the poor prognosis of acute myeloid leukemia (AML) patients, but the underlying mechanism remains poorly understood. Given the unique microenvironment of bone marrow, we reasoned that drug resistance of AML might rely on distinct metabolic processes. Here, we identify succinate dehydrogenase (SDH) deficiency and over-cumulative succinate as typical features in AML, with a marked function in causing the resistance of AML cells to various anti-cancer therapies. Mechanistically, succinate promotes the accumulation of oncogenic proteins in a manner that precedes transcriptional activation. This function is mediated by succinate-triggered upregulation of ubiquitin-conjugating enzyme E2M (UBC12) phosphorylation, which impairs its E2 function in cullins neddylation. Notably, decreasing succinate by fludarabine can restore the sensitivity of anti-cancer drugs in SDH-deficient AML. Together, we uncover the function of succinate in driving drug resistance by regulating p-UBC12/cullin activity, and indicate reshaping succinate metabolism as a promising treatment for SDH-deficient AML.

Acute myeloid leukemia (AML) is an aggressive hematological malignancy, and drug resistance is closely intertwined with its poor prognosis, resulting in a 5-year survival rate of only 27%¹. While some studies have investigated drug resistance mechanisms in AML, they offer limited insights and poor progress in overcoming clinical drug resistance². The bone marrow microenvironment causes AML cells to rely on distinct metabolic pathways, making them susceptible to metabolic changes³. Metabolic alterations not only fulfill the increased energy requirements of cancer cells⁴, but also provide rapid defense against external stresses⁵. It is of interest to investigate how metabolic alterations influence the AML drug sensitivity.

Succinate dehydrogenase (SDH), isocitrate dehydrogenase (IDH), and fumarate hydratase (FH) are classical tumor suppressors in the tricarboxylic acid (TCA) cycle. When mutant or down-regulated, they contribute to tumor progression by causing the accumulation of oncometabolites^{6–8}. Among them, *IDH* mutations are closely associated with the progression in around 20% of AML patients and are well therapeutically exploited^{9,10}. This inspired us to explore whether *SDH* or *FH* alterations also play a role in AML, which is largely unknown. SDH deficiency, which leads to succinate accumulation, is frequently deficient in solid tumors and associated with poor prognosis^{11,12}. Interestingly, SDH deficiency has been associated with imatinib resistance in

¹Institute of Pharmacology and Toxicology, Zhejiang Province Key Laboratory of Anti-Cancer Drug Research, College of Pharmaceutical Sciences, Zhejiang University, Hangzhou, China. ²Division of Hematology-Oncology, Children's Hospital, Zhejiang University School of Medicine, National Clinical Research Center for Child Health, Hangzhou, China. ³Engineering Research Center of Innovative Anticancer Drugs, Ministry of Education, Hangzhou, China. ⁴Cancer Center, Zhejiang University, Hangzhou, China. ⁵These authors contributed equally: Yifan Chen, Miao Xian. ✉e-mail: mying@zju.edu.cn

gastrointestinal stromal tumor (GIST) patients¹³, which raises the intriguingly possible correlation between SDH deficiency and drug resistance. However, the relationship between SDH deficiency and drug resistance in cancer cells remains poorly understood.

Although the currently reported tumor-promoting mechanisms of SDH deficiency and succinate are very similar with *IDH/FH* alterations, mainly through inhibiting alpha-ketoglutarate (α KG)-dependent dioxygenase, thus activating HIF1 α ^{14,15}, it fails to explain all the primitive and rapid adaptation of tumor cells to exogenous stresses¹⁴. Additionally, HIF1 α has also been found to act as a tumor suppressor, especially in AML^{16,17}. Therefore, it is necessary to identify other oncogenic mechanisms associated with SDH deficiency. In mammals, approximately 20% of proteins undergo constant synthesis and degradation, with the degradation process being regulated by ubiquitination mediated by cullins¹⁸. It is crucial for the proper functioning of cells to maintain homeostatic levels of these proteins, particularly oncoproteins, to promote malignant phenotypes. Post-translational modifications (PTMs), such as cullin-ring-ligases (CRLs)-mediated ubiquitination can rapidly modulate abundant proteins stability¹⁹. In this context, we are curious that in addition to transcriptional activation, whether the rapid PTM-mediated regulation of proteins may play a role in the ability of succinate and other onco-metabolites to enable tumor cells to counteract external stressors.

Here, we have identified SDH was frequently deficient in AML, highly possibly caused by transcription downregulation or gene mutations. SDH deficiency-driven succinate accumulation can lead to the resistance of AML cells to various anti-cancer therapies. We discovered that UBC12, one of the two essential E2 enzymes involved in neddylation, can be phosphorylated. This phosphorylation, enhanced by succinate, negatively regulates the E2 enzyme activity of UBC12 and cullins neddylation, thus comprehensively modulating oncoproteins homeostasis like WEE1, which plays an important role in the drug resistance induced by SDH deficiency. This function of succinate in promoting protein stability provides AML cells with a rapid defense mechanism against anti-cancer therapies. Moreover, we have demonstrated that reshaping dysregulated succinate metabolism by fludarabine significantly inhibits SDH-deficient AML both in vitro and in vivo, and low concentrations of fludarabine can effectively enhance the anti-cancer effects of the first-line drugs in AML treatment. Thus, we uncover that SDH deficiency could serve as a potential molecular subtype of AML that exhibits drug resistance, and propose that blunting the metabolic collapse of succinate may generate an effective strategy to overcome the clinical drug resistance in SDH-deficient tumors.

Results

SDH deficiency is a common characteristic of AML and is closely associated with a broad spectrum of drug resistance

To explore whether SDH or FH alterations also play a role in AML, we first compared the mutation rates of *SDH* and *FH* with the typical mutated *IDH* gene. *SDHx* (*SDHA-SDHD*) mutation was detected in 30.67% of AML patients (50/163), and all of them contained *SDHA* mutations. It occurred more frequently than *IDH1/2* mutations (19.02%) or *FH* mutations (2.45%) (Figs. 1a and S1a). Notably, 11.04% of AML patients (18/163) displayed co-occurrence of *SDHx* and *IDH1/2* mutations. 18 *SDHA* mutation sites were identified in AML cells, with 9 of them also identical to be the mutation sites in pheochromocytoma and paraganglioma (PCPG), the classic *SDH* mutant cancer type (Table S1, S2). Loss-of-function mutations and significantly reduced mRNA levels could contribute to SDH deficiency. Subsequently, we delved deeper into SDH deficiency by examining mRNA levels in AML. Indeed, the expression levels of *SDHx*, as well as *IDH1/2* and *FH*, were significantly lower in AML patients compared to normal tissue, indicating their inability to function as tumor suppressors (Fig. 1b). Similar phenomenon was observed in PCPG, cholangiocarcinoma (CHOL),

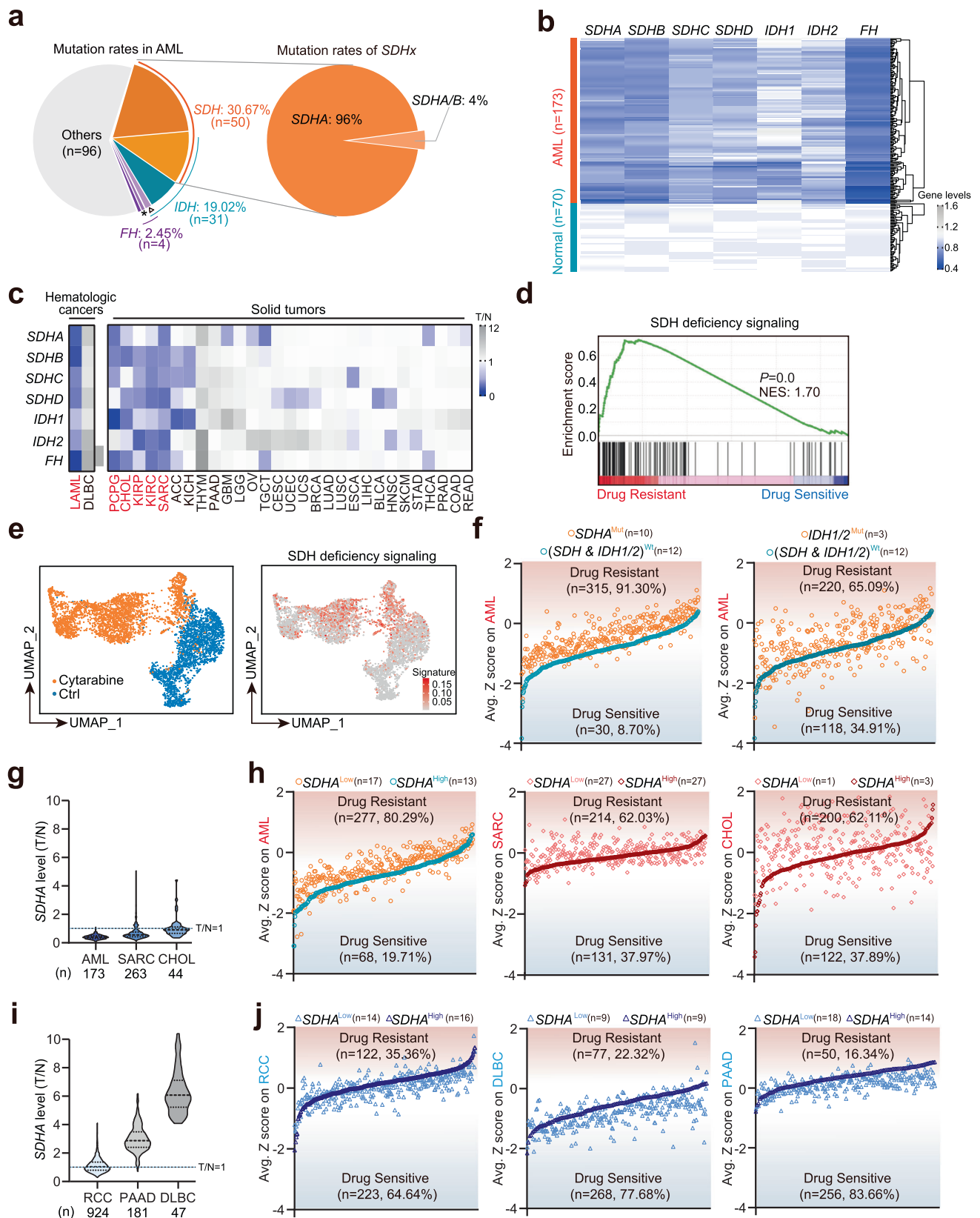
renal cell carcinoma (RCC) and Sarcoma (SARC), where SDH deficiency has been implicated as a key driving factor (Fig. 1c, Table S3). In addition, there is a significant positive correlation between *SDHA* mRNA levels and SDHA protein levels in primary AML samples, indicating that low mRNA levels of *SDH* also can result in decreased protein levels (Fig. S1c). Besides, most AML patients with *SDHA* mutations also have lower SDHA protein levels. These results indicate that comparing to *IDH* mutation, *SDH* is more frequently deficient in AML cells.

We then investigated the correlation between SDH deficiency and drug sensitivity in AML. We found that SDH deficiency-associated gene set was significantly enriched in the transcriptome of drug resistant leukemia cells (Fig. 1d). Moreover, single-cell RNA-seq data showed that SDH deficiency-associated genes were highly expressed in primary AML cells that survived after cytarabine treatment (Fig. 1e). These results suggest that SDH deficiency may play an important role in the self-protection of AML cells against anti-cancer therapies. Since we found that gene mutations and transcriptional downregulation may lead to SDH deficiency in AML, we next examined the drug sensitivity of AML samples with *SDH* mutant or *SDH* low mRNA expression. For *SDH* mutant samples, considering that *SDHA* mutation occurs at the highest rate among the four subunits of *SDH* in AML patients, we focused on *SDHA* mutant to investigate SDH deficiency in our subsequent investigation. We classified AML cell lines into *SDHA*^{Mut} and *SDHx*^{Wt} groups, and then analyzed their sensitivity to over 300 FDA approved anti-cancer drugs. Higher Z scores indicate higher drug resistance. We found that *SDHA*^{Mut} group exhibited higher Z scores for 91.30% of the drugs, indicating potential drug resistance (Fig. 1f, Table S4). The *IDH1/2* mutation group showed a drug resistance rate of 65.09%, and for AML cells with *SDHA* plus *IDH1/2* mutations, this proportion was 94.97%, slightly higher than 91.30%, suggesting that *IDH1/2* mutations may weakly enhance drug resistance in AML cells with *SDH* mutations, but the overall impact is not significant (Figs. 1f, S1d and Table S5). These data suggest that *SDHA* mutation is highly correlated with drug resistance in AML.

For *SDH* low mRNA expression samples, we evaluated the correlation between SDHA expression levels and drug sensitivity in various cancer types. Among them, SARC, CHOL as well as AML were selected as they exhibited significantly lower *SDHA* expression. Specifically, the tumor-to-normal tissue (T/N) ratios of *SDHA* expression were predominantly less than 1 (Fig. 1g). AML cell lines were then classified into *SDHA*^{Low} group and *SDHA*^{High} group based on the average mRNA levels of *SDHA*. The Z scores of AML cell lines in the *SDHA*^{Low} group for most drugs (80.29%) were higher than those in the *SDHA*^{High} group. Similar findings were also observed in SARC and CHOL (Fig. 1h). By contrast, in those tumors where the majority of the T/N ratios of *SDHA* expression were greater than 1, the majority of Z scores in the *SDHA*^{Low} group were lower than those in the *SDHA*^{High} group (Fig. 1i, j). The above evidences indicate that only when the expression of *SDHA* is severely low, leading to its deficiency, lower expression positively correlates with drug resistance in cancer cells. Collectively, our results indicate that SDH deficiency, either caused by low expression or mutations, can cause wide-ranging drug resistance in tumor cells, particularly in AML.

Succinate accumulates in SDH-deficient AML and drives drug resistance

SDH deficiency could induce abnormal accumulation of succinate²⁰. Therefore, we subsequently analyzed the succinate levels in AML models and its correlation with SDH deficiency. We first evaluated succinate levels in patient-derived AML cells (PDCs). As expected, AML blasts with lower mRNA levels or protein levels of SDHA exhibited higher succinate content (Figs. 2a, S2a). We defined primary AML cells as the *SDHA*^{Low} group and *SDHA*^{High} group based on SDHA protein expression and found that the average succinate content in the *SDHA*^{Low} group is 2.16 times than that of the *SDHA*^{High} group, comparable to the fold increase observed in succinate levels following SDHA



knockdown in cell lines (Fig. S2b, c). Moreover, we compared succinate levels in primary bone marrow from AML patients with those from non-AML normal donors. AML blasts exhibited elevated succinate levels than normal blasts, where succinate levels were 810.93 ± 400.61 nmole/ 10^6 cells in AML patients v.s. 313.59 ± 112.35 nmole/ 10^6 cells in non-AML control, representing a more than two-fold increase (Fig. 2b,

left). Given the potential secretion of succinate from cells into the extracellular milieu, succinate levels were additionally assessed in bone marrow plasma obtained from AML patients. It was observed that succinate levels in the bone marrow plasma of AML patients were significantly elevated compared to the control group (Fig. 2b, right). Similarly, succinate levels in both bone marrow and peripheral blood

Fig. 1 | SDH deficiency is a common characteristic of AML and is closely associated with a broad spectrum of drug resistance. **a** The mutation rates of *SDHx*, *IDH1/2* and *FH* in AML. The raw data is sourced from TCGA. *represents AML samples with both *FH* and *SDH* mutations. Δ represents AML samples with both *FH* and *IDH* mutations. **b** The expression of *SDHx*, *IDH1/2* or *FH* in AML samples and normal tissues. **c** The ratios of the median expression of *SDHx*, *IDH1/2* or *FH* in different cancer species (T) compared to their corresponding normal tissues (N). The full names of different tumors were listed in the Supplementary table 1. **b, c** The gene expression data for different cancer species, including AML, was obtained from TCGA, while those for normal tissues were sourced from GTEx. The above data were downloaded from the ‘A combined cohort of TCGA, TARGET, and GTEx samples’ dataset on the UCSC Xena (<https://xena.ucsc.edu/>). **d** GSEA enrichment plot for SDH deficiency signaling in drug resistant K562 vs drug sensitive K562. (Data of K562 transcriptome is from GSE131823). SDH deficiency signaling is defined by GSEA’s official “CERVERA_SDHB_TARGETS_1_UP” set. The significance

analysis was conducted by two-tailed unpaired Student’s *t*-test. **e**, UMAP plot of control (blue; *n* = 1952) and cytarabine-treated AML cells (orange, *n* = 2675) (Left). UMAP plot displaying the signature scores for SDH deficiency signaling (Right). (Single-cell RNA-seq data is from GSE146590). **f–j** The relationship between genes expression or mutation and drug sensitivity in diverse tumor cells. The *SDHA*^{Mut} group does not include cells with *IDH1/2* mutations, and vice versa for the *IDH1/2*^{Mut} group. The (*SDH* & *IDH1/2*)^{WT} group includes cells that do not have mutations in *SDH* and *IDH1/2*. Indicated tumor cells with higher-than-average of *SDHA* expression values were classified into the *SDHA*^{high} group, and the opposite were classified into the *SDHA*^{low} group. Z scores of anticancer drugs on tumor cells in the same group were averaged and marked by different colors. The T/N ratios of *SDHA* level were exhibited in Fig. 1f, h. T: tumor; N: normal. RCC includes kidney renal papillary cell carcinoma (KIRP) and kidney renal clear cell carcinoma (KIRC). Source data are provided as a Source Data file.

of AML-bearing mice were significantly higher than those of non-AML-bearing mice (Figs. 2c, S2d). These results indicate that AML cells exhibit a distinctive metabolic feature characterized by elevated succinate levels, likely attributed to SDH deficiency. We also detected the IC₅₀ values of the first-line chemotherapies on PDCs, and found a significant association between elevated succinate levels and higher IC₅₀ values for the most first-line chemotherapies (Fig. 2d). Similarly, lower *SDHA* mRNA levels correspond to higher resistance indices of primary AML cells to these chemotherapies (Fig. S2e). These results indicate that succinate accumulation was strongly correlated with the reduced drug sensitivity in AML cells.

We next investigated whether manipulating the levels of SDHA, resulting in aberrant succinate accumulation, could achieve its canonical pro-oncogenic effects in AML cells. SDHA was knocked down in HL-60 cells to establish a model with high succinate level (Fig. 2e). In line with previous findings in solid tumors^{21,22}, SDHA knockdown in AML cells exhibited an enhancement in clone formation abilities, similar to the effect observed with succinate treatment (Fig. 2f, g). To investigate whether SDH deficiency can similarly promote AML progression in vivo, we evaluated the effect of SDHA knockdown on tumor growth in HL-60 subcutaneous xenograft mouse models. As expected, the tumor growth rate was significantly accelerated in the two shSDHA groups compared to the shCtrl group (Fig. 2h, i). These results indicate that succinate accumulation could enhance the malignancy of AML cells, paralleling its tumor-promoting effects in solid tumors.

We further examined whether SDHA knockdown could elicit a novel function of inducing drug resistance in AML. We treated AML cells with gradient concentrations of first-line chemotherapeutic drugs and found SDHA knockdown could significantly induce AML resistance to 72.73% of chemotherapies (8/11) (Fig. 2j). Strikingly, SDHA knockdown could also obviously trigger AML resistance to 88.89% of targeted drugs (64/72) (Fig. 2k), suggesting that SDHA knockdown-caused drug resistance is broad-spectrum across multiple drugs. Furthermore, supplementing SDHA in cells with low SDHA expression can effectively reverse the drug resistance induced by SDHA deficiency (Fig. S2f, g). Therefore, we can conclude that SDH deficiency caused abnormal succinate accumulation in AML, which could promote tumor progression in vitro and in vivo as well as provoking AML cell resistance to broad anti-cancer drugs, probably contributing to the poor prognosis of AML patients.

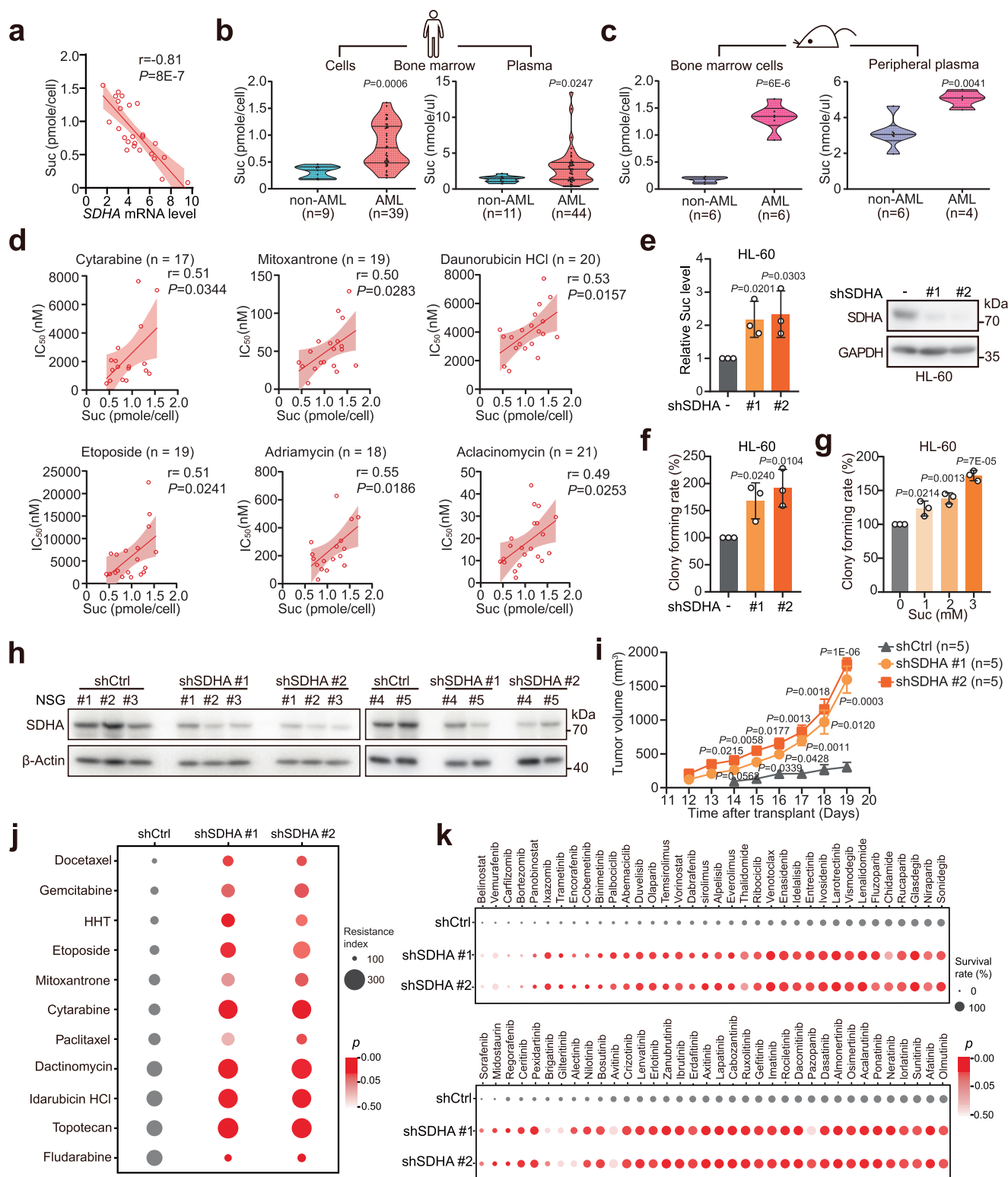
Succinate impairs the E2 enzyme function of UBC12 to enhance the stability of tumor-promoting proteins

Considering that succinate can induce AML resistance to various types of anti-cancer drugs, we speculate that succinate might possess a broad and rapid regulatory mechanism for a diverse range of substrates. To explore this, HL-60 cells were treated with succinate for 3 h

or 24 h, followed by proteome and transcriptome sequencing. Proteome analysis showed that 255 proteins (cluster I+II) were upregulated after succinate treatment (Fig. 3a). Among these 255 proteins, the majority did not exhibit an increase in their corresponding transcription levels at either 3 h or 24 h after succinate treatment, while a small portion showed an increase in transcription levels at 24 h, indicating that the upregulation of proteins in succinate-treated cells was not solely attributed to increased transcription (Fig. 3b). These results reveal the function of succinate in modulating protein homeostasis, which appears to be more rapid than transcriptional regulation. We then investigate whether succinate-upregulated proteins contribute to drug resistance and tumor progression. Firstly, we observed that oncogenic signaling pathways, like E2F, G2M and MYC signaling, were significantly enriched in the succinate treatment group (Fig. 3c), which has been identified to be closely related with tumor progression and drug resistance^{23,24}. Then, 34 proteins that upregulated by succinate in the above signaling were overlapped with the 255 proteins (cluster I+II), among which the high expression of WEE1 and TUBG1 were identified to be significantly associated with the low survival rates of AML patients. It has been widely reported that WEE1 play an important role with the drug resistance of cancer cells^{25,26}. Additionally, proteomics data indicate that the upregulation of WEE1 by succinate is higher than that of TUBG1 (Fig. 3d). Therefore, we next primarily investigate the role of WEE1 in SDH deficiency-induced drug resistance. We confirmed that succinate treatment indeed upregulated the protein level of WEE1 without altering its transcript levels (Fig. 3e). Furthermore, knocking down WEE1 in SDHA knocked down HL-60 cells could reverse the drug resistance caused by SDH deficiency (Fig. 3f, g). These findings suggest that the accumulation of oncogenic proteins like WEE1 regulated by the p-UBC12/cullin pathway due to SDH deficiency may play a critical role in the drug resistance process in AML.

We next investigated the molecular mechanisms underlying succinate-induced accumulation of oncogenic proteins. GSEA analysis revealed that the protein set associated with neddylation inhibitor MLN4924 treatment²⁷ and proteasome inhibitors MG132 treatment²⁸, but not autophagy inhibitor CQ treatment²⁹, were significantly enriched after 3 h and 24 h succinate treatment (Fig. 3h). CRLs are activated by neddylation modification, mainly functioning as E3 ligases in ubiquitination¹⁸. This led us to speculate succinate may enhance protein stability through inhibiting cullins neddylation. Moreover, succinate significantly impaired cullins neddylation (Fig. 3i), and knockdown of SDHA exerted similar effects (Fig. 3j). These results indicate that succinate has an inhibitory effect on neddylation, which may strongly enhance protein stability.

Neddylation is a cascaded enzyme reaction, which is regulated by E1/E2/E3 enzymes. We next explored whether succinate could block the cascaded enzyme reaction to inhibit neddylation. The result illustrated that succinate treatment inhibited the interaction between



neddylating E2 enzyme UBC12 and E1 enzyme, NEDD8 activating enzyme (NAE), which is formed by the heterodimerization of UBE1C and NAE1 (Fig. 3k). Succinate pre-treatment also inhibited UBC12 binding to recombinant UBE1C (Fig. 3l), indicating that succinate could impact UBC12 activity, rather than UBE1C. Overall, these findings demonstrated that succinate mediates rapid and ubiquitous drug resistance in AML cells, mainly through increasing substantial tumor-promoting proteins by attenuating the function of UBC12 and inhibiting cullins neddylation.

Succinate promotes the phosphorylation of UBC12 at serine-6 site through PKC α

Post-translational modifications (PTMs) provide a rapid response to stimuli, finely tuning metabolism and protein expression. Since succinate can rapidly cause protein accumulation by inhibiting UBC12 function, we hypothesized that succinate may modulate UBC12 function by affecting its PTMs. We screened a panel of PTM inhibitors and found phosphatase enzyme inhibitor calyculin A could most effectively inhibit cullin 3 neddylation (Fig. S3a), indicating phosphorylation

Fig. 2 | Succinate accumulates in SDH-deficient AML and drives drug resistance. **a** Correlation analysis between *SDHA* mRNA levels and succinate levels in primary AML samples ($n = 25$). **b** The succinate levels of cells and plasma in the bone marrow of primary AML sample and non-AML samples. **c** The succinate levels of bone marrow cells and peripheral plasma in AML orthotopic xenograft mice and normal mice. **d** Correlation analysis between IC_{50} of different chemotherapy drugs on primary AML samples and the succinate levels of these samples. **a, d** Pearson correlation coefficient r was calculated by GraphPad Prism. Data are presented as mean \pm 95% confidence bands. The significance analysis was conducted by simple linear regression. **e** SDHA was knocked down in HL-60 cells using lentiviral infection, followed by two rounds of puromycin selection to establish stable SDHA knock-down cell lines. Then the succinate levels of HL-60 shCtrl cells and HL-60 shSDHA cells, and the effects of SDHA knock down were detected. The HL-60 shCtrl and HL-60 shSDHA cells used in the following are the same as the cells used here. **(f)** The

clone formation rates of shCtrl cells and shSDHA HL-60 cells. **g** The clone formation rates of HL-60 cells after treated with different concentrations of succinate for 10–14 days. Suc: succinate. **h** The effect of SDHA knocked down in the tumors of AML xenograft models. **i** Tumor growth of the shCtrl and shSDHA HL-60 cells derived xenografts in NSG mice. Tumor volume growth curves are based as mean \pm SE ($n = 5$). **j, k** shCtrl and shSDHA HL-60 cells were treated with three gradient concentrations of chemotherapy drugs (**j**) or 50% peak plasma concentration (PPC) of targeted drugs for three days (**k**). The resistance index is calculated using the area under the curve (AUC) of cell viability at three chemotherapy drug concentrations. A larger resistance index indicates greater drug resistance. **b–c, e–g**, Data are presented as mean \pm SD; **(b–c, e–g, i–k)** The significance analysis was conducted by two-tailed unpaired Student's t -test. **e–g** Three independent experiments were performed. Source data are provided as a Source Data file.

may regulate UBC12 activity. Our subsequent experiments revealed that UBC12 can indeed undergo phosphorylation, as evidenced by the detection of phosphorylation signals (Ser/Thr), which were diminished by calf intestinal alkaline phosphatase (CIAP) treatment (Fig. 4a). Furthermore, both succinate treatment (Fig. 4b) and calyculin A treatment (Fig. S3b) dramatically increased Ser/Thr phosphorylation of UBC12. Using Phos-tag, which selectively separates phosphorylated protein from the non-phosphorylated counterparts on SDS-PAGE³⁰, we observed a distinct band corresponding to phosphorylated UBC12 (Fig. S3c). Additionally, we did not detect any tyrosine phosphorylation signal of UBC12 with the tyrosine phosphatase inhibitor Na_3VO_4 treatment (Fig. S3d). Collectively, these findings confirm that UBC12 can undergo phosphorylation at serine Ser/Thr sites, which can be further enhanced by succinate.

To identify the phosphorylation sites of UBC12, we conducted two independent mass spectrometry experiments. S6, S28, and S175 were detected as potential phosphorylation sites of UBC12 in both experiments, while S50 and S73 were potential sites in one experiment each (Figs. S3e, S3e). Further mutational analysis of above sites indicated S6 is the preferential phosphorylation site for UBC12 (Fig. 4d). Moreover, different mutant types at S6 did not show phosphorylated signals under calyculin A treatment or phos-tag system (Figs. 4e, f, S3f,g). We then generated a custom-made anti-UBC12 (phosphor S6) antibody, and confirmed that UBC12 can indeed be phosphorylated at S6 site. Additionally, both succinate treatment and SDHA knockdown increased UBC12 phosphorylation at S6 (Fig. 4g,h). These findings validate that UBC12 undergoes phosphorylation at site 6, and succinate further enhances its phosphorylation.

To elucidate the mechanism underlying UBC12 phosphorylation, we predicted the potential phosphokinases of UBC12 on NetPhos 3.1, and identified PKC as the most likely candidate. Our experimental findings demonstrated that PKC activator TPA treatment increased UBC12 phosphorylation (Figs. 4i, S4a). Additionally, inhibition of PKC using specific inhibitors attenuated UBC12 phosphorylation (Fig. S4b–f), indicating that PKC can phosphorylate UBC12. To further investigate which PKC isoform is responsible for UBC12 phosphorylation, we generated PKC α -CAT, which retained only the catalytic domain (CAT) of PKC, and PKC α -CAT-DN, which contained a point mutation abolishing ATP binding ability. Overexpression of PKC α -CAT resulted in a noticeable increase in UBC12 phosphorylation (Figs. 4j, S5a), while PKC α -CAT-DN had no influence on phosphorylation (Fig. 4k). Importantly, while PKC α -CAT promoted the phosphorylation of UBC12^{WT}, no increase in phosphorylation was detected in the S6 mutant UBC12 (Figs. 4l, S5b). In contrast, PKC β and its variants exhibited either no effect or a weaker effect on UBC12 phosphorylation compared to PKC α (Fig. S5c,d). An in vitro PKC α kinase assay confirmed that PKC α , not PKC β , phosphorylated UBC12 at S6 (Figs. 4m, S5e). Finally, we observed that PKC inhibitor treatment significantly decreased succinate-induced phosphorylation of UBC12 at S6 (Fig. 4n), further supporting PKC α as the specific phosphokinase responsible for

UBC12 phosphorylation at S6. In summary, these findings collectively demonstrate that succinate promotes the phosphorylation of UBC12 at S6 site through PKC α activation.

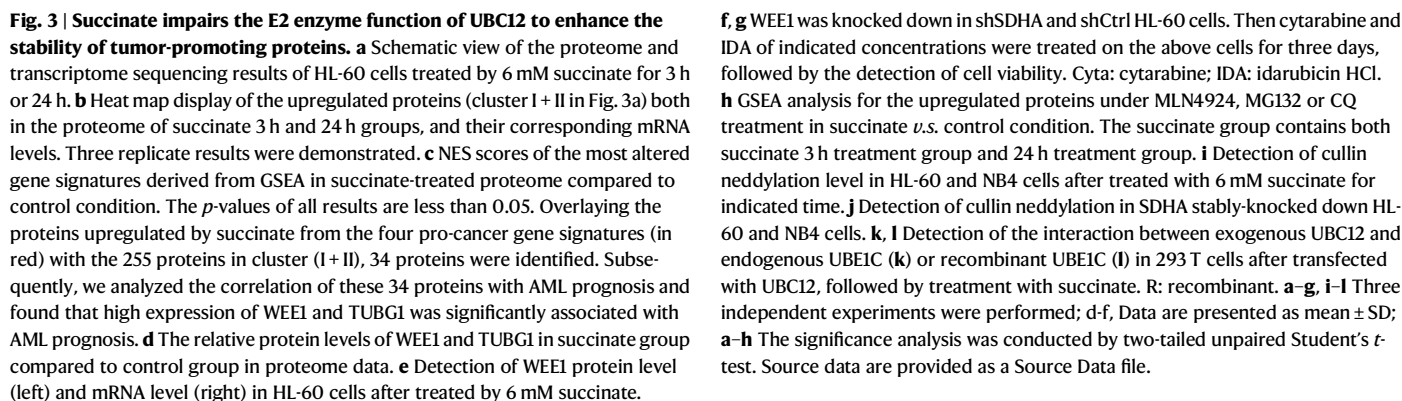
Phosphorylation of UBC12 impairs cullins neddylation through disrupting UBC12/UBE1C interaction

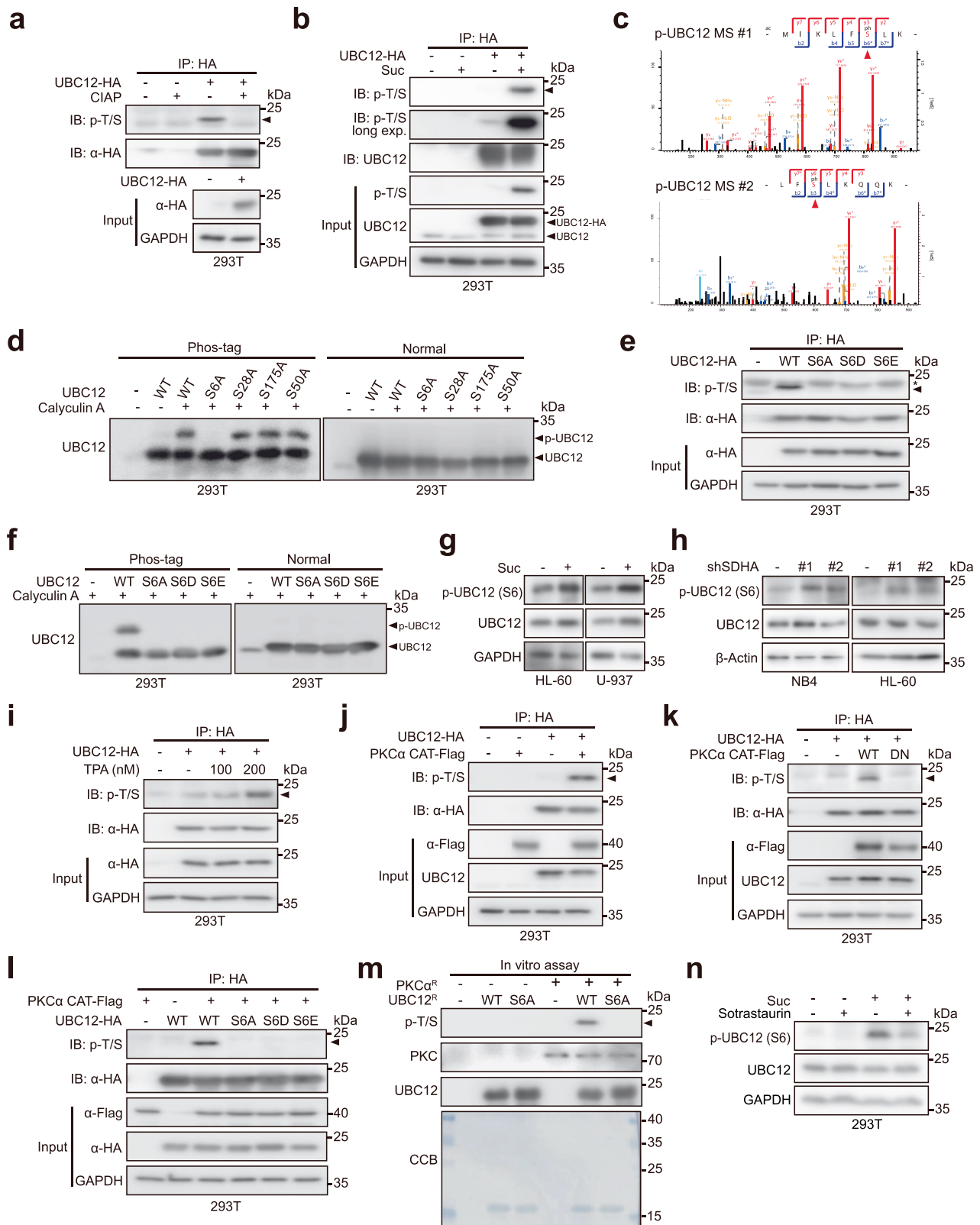
We next explored whether phosphorylation of UBC12 would affect its E2 enzyme function. We found while both UBC12^{WT} and UBC12^{S6A} (mimicking hypo-phosphorylation) could interact with E1 enzyme UBE1C, UBC12^{S6D} and UBC12^{S6E} (both simulating hyperphosphorylation) exhibited significantly weaker interaction with UBE1C (Figs. 5a, S6a,b). Interestingly, the mutation at S6 did not influence the interaction between UBC12 and the neddylation E3 enzyme DCN1 (Figs. 5b, S6c). Furthermore, calyculin A treatment hindered the UBC12/UBE1C interaction and this inhibition was further enhanced by the addition of TPA treatment (Figs. 5c, S6d). Moreover, PKC α -CAT overexpression also reduced UBE1C/UBC12 interaction, which was rescued by the PKC inhibitor sotrastaurin (Fig. 5d), suggesting phosphorylation of UBC12 inhibit its interaction with neddylation E1 enzyme UBE1C, rather than E3 enzyme DCN1.

To better characterize the effect of hyperphosphorylated UBC12 on the neddylation pathway, we detected NEDD8 transfer ability of UBC12^{WT} and UBC12^{S6A/S6D/S6E} in vitro. While UBC12^{S6A} exhibited similar NEDD8 transfer activity to UBC12^{WT}, UBC12^{S6D} and UBC12^{S6E} showed reduced NEDD8 transfer (Fig. 5e,f). In addition, overexpression of UBC12^{WT} and UBC12^{S6A} could increase the neddylation of cullin 1 and cullin 3, whereas UBC12^{S6D} and UBC12^{S6E} did not exhibit the same effect (Fig. 5g). Moreover, calyculin A treatment impaired cullins neddylation, which was further promoted by PKC α overexpression (Fig. 5h). Taken together, our findings suggest that phosphorylation of UBC12 impairs NEDD8 transfer and cullins neddylation. The role of succinate in upregulating UBC12 phosphorylation provides an explanation for its ability to inhibit cullin neddylation and promote the accumulation of the CRLs downstream oncoproteins.

Reshaping succinate metabolism by fludarabine can antagonize drug resistance in AML cells

Given that succinate accumulation induced multidrug resistance, it is plausible that restoring succinate metabolism may potentially recover drug sensitivity. To identify effective strategies for reducing succinate levels, we conducted a screening of an FDA-approved anticancer drug library and found that seven drugs exhibited more than a 50% suppression in succinate levels (Fig. 6a). Further investigation identified that among these drugs, fludarabine exhibited the most potent inhibitory effect (Fig. 6b). Fludarabine is a purine nucleoside analog that exerts antineoplastic effect primarily through inhibiting DNA synthesis³¹. Here, we observed fludarabine treatment effectively reversed the succinate increase induced by SDHA knockdown (Fig. 6c), and restored the upregulated UBC12 phosphorylation (Fig. 6d) and inhibited cullins neddylation caused by succinate





treatment (Fig. 6e). These results indicate that fludarabine can effectively decrease succinate levels and antagonize the inhibitory effect of succinate on neddylation.

We next explored whether reshaping succinate metabolism through fludarabine treatment could specifically inhibit the malignant phenotypes of SDH-deficient AML cells. Compared to shCtrl cells, fludarabine exhibited a more pronounced inhibitory effect on the

proliferation of shSDHA cells (Fig. 6f). CB-839, which can reduce succinate levels, exhibits similar efficacy but demonstrated weaker inhibition of shSDHA cells compared to fludarabine (Fig. 6g). Moreover, fludarabine exhibited a more effective inhibition of clone formation in shSDHA cells compared to shCtrl cells (Fig. 6h). Consistently, a higher percentage of apoptotic cells was observed in shSDHA cells treated with fludarabine compared to shCtrl cells (Fig. 6i). To exclude the

Fig. 4 | Succinate promotes the phosphorylation of UBC12 at serine-6 site through PKC α . **a, b** Detection of the Ser/Thr phosphorylation level of UBC12 in 293 T cells after transfected with UBC12, followed by treatment with CIAP (**a**) or succinate (**b**). **c** Second order spectra of UBC12 S6 in two independent mass spectrometry experiments. **d–f** Detection of the phosphorylation level of UBC12^{WT} and different mutant UBC12 in 293 T cells after treated by 25 nM calyculin A for 1.5 h. **g** Anti-UBC12 (phospho S6) antibody was customized and used to detect the phosphorylation level of UBC12 in HL-60 and U-937 cells after treated with 6 mM succinate for 3 days. **h** Detection of the phosphorylation level of UBC12 in HL-60 and NB4 cells after SDHA was stably knocked down. **i** Detection of the phosphorylation level of UBC12 in 293 T cells after transfected with UBC12, followed by treatment with different concentrations of TPA for 45 min. **j–k** Detection of the phosphorylation level of UBC12 in 293 T cells after transfected with UBC12 and

PKC α CAT (**j**), or UBC12, PKC α CAT and PKC α CAT DN (**k**). **l** Detection of the phosphorylation level of UBC12^{WT} and different mutant types at S6 of UBC12 in 293 T cells after transfected with PKC α CAT. **m** Detection of the phosphorylation level of recombinant UBC12^{WT} or UBC12^{S6A} proteins after incubated with recombinant PKC α protein. **n** Pre-treat HL-60 cells with 200 nM sotrastaurin for 24 h, then treat with 6 mM succinate for 2 days, followed by detecting the phosphorylation levels of UBC12. **a–b, e, i–l** and **m** The samples derive from the same experiment but different gels for p-T/S and another for α -HA or UBC12 were processed in parallel. **d** and **f**, The samples derive from the same experiment but Phos-tag SDS-PAGE and normal SDS-PAGE were used in parallel to detect UBC12 and p-UBC12. **g, h** and **n**, The samples derive from the same experiment but different gels for p-UBC12 and another for UBC12 were processed in parallel. Source data are provided as a Source Data file.

classic DNA synthesis inhibition effect of fludarabine from its impact on killing shSDHA cells, we treated shSDHA cells with gradient concentrations of fludarabine and then measured intracellular succinate levels as well as cell viability (Fig. 6j). The results showed that fludarabine, at low concentrations of 50–200 nM, could downregulate succinate levels without significantly inhibiting cell viability. At a concentration of 300 nM, succinate levels did not decrease further, but cell viability was significantly reduced. We also investigated whether low concentration of fludarabine could synergistically enhance the inhibitory effect of other antitumor drugs (Fig. 6k,l). The results showed that when cytarabine and idarubicin HCl were used alone, the shSDHA groups exhibited resistance to these drugs compared to the control group. However, when cytarabine or idarubicin HCl was combined with low concentration of fludarabine, their anti-tumor effects were significantly enhanced. These results suggest that low concentrations of fludarabine do not kill AML cells but can enhance the sensitivity to other drugs by downregulating succinate levels. At higher concentrations, both the inhibition of succinate and DNA synthesis contribute to the antitumor effects of fludarabine.

Fludarabine specifically inhibits SDH-deficient AML in both primary samples and in vivo models

We next investigated the potential of fludarabine as an effective therapy for SDH-deficient AML. We determined the IC₅₀ of fludarabine on primary AML cells and observed a striking correlation between higher succinate levels and lower IC₅₀ values of fludarabine (Fig. 7a), indicating that fludarabine specifically inhibits primary AML cells with high succinate levels. To evaluate the therapeutic effect of fludarabine on SDH-deficient AML in vivo, shSDHA or shCtrl HL-60 cells were used to establish xenograft models, followed by treatment with fludarabine, as well as cytarabine serving as a control (Fig. 7b). Both cytarabine and fludarabine could inhibit the tumor growth of shCtrl group, with inhibition rates of 52.47% and 84.34%, respectively. However, cytarabine had minimal impact on the tumor growth in the shSDHA group, whereas fludarabine obviously inhibited the tumor growth in the shSDHA group by 82.64% (Fig. 7c–e). These data demonstrate that SDH deficiency can lead to drug resistance in AML cell in vivo, but fludarabine retains the ability to effectively suppress their growth. Additionally, fludarabine was also found to significantly decrease succinate levels in tumor tissues derived from shSDHA cells, while cytarabine had no effect on succinate levels (Fig. 7f), indicating that reshaping succinate metabolism makes a significant contribution to the inhibitory effect of fludarabine.

Furthermore, we evaluated whether fludarabine could improve the prognosis of AML patient-derived xenograft (PDX) with high succinate levels. Remarkably, fludarabine significantly extended the survival time of these AML PDX mice, while cytarabine did not show any significant difference compared to the control group (Fig. 7g). Taken together, these findings illustrate that reshaping succinate metabolism by fludarabine can effectively inhibit SDH deficient AML in both in vivo

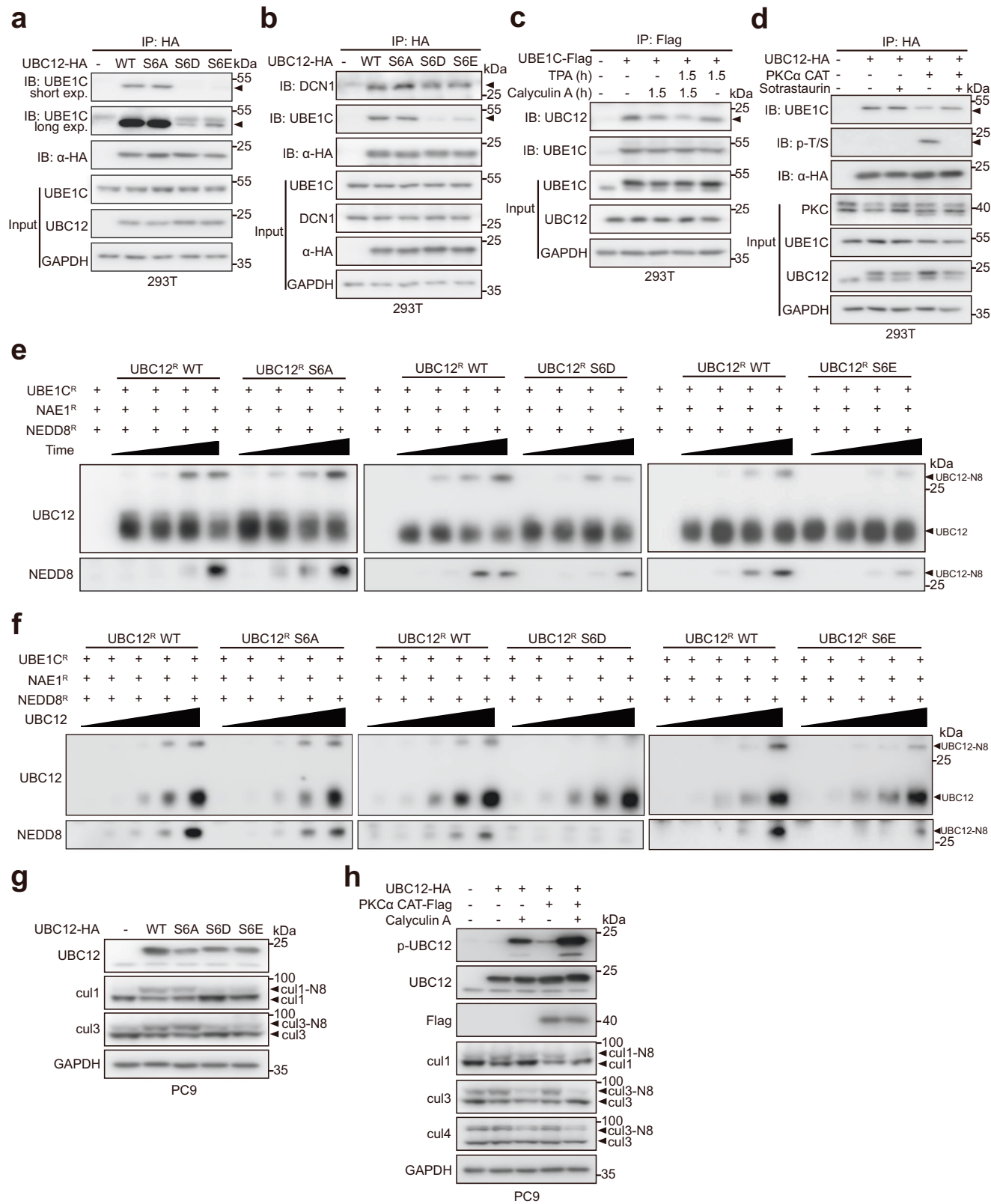
models and primary samples, provides fludarabine as an attractive therapeutic strategy for the treatment of SDH-deficient AML in clinical practice.

Discussion

SDH deficiency is linked to poor prognosis in solid tumors, but limited research has investigated its role in drug sensitivity and AML. In this study, we identified that transcription downregulation or gene mutations could highly possibly lead to the frequent deficiency of SDH in AML. We demonstrated that the accumulation of oncometabolite succinate caused by SDH deficiency is the critical reason contributing to drug resistance in AML cells. We proposed that succinate activated p-UBC12/cullin pathways, rapidly regulating oncoprotein homeostasis as a first-line defense for AML cells against anticancer agents. Given the important function of accumulated succinate in modulating drug sensitivity, we suggested that reshaping succinate metabolism could help overcome drug resistance in SDH-deficient tumors like AML.

Oncometabolites abnormally accumulate when TCA cycle enzymes are altered, and although their tumor-promoting role is well-established, their correlation with drug resistance remains uncertain. Gene alterations have long-identified as a common mechanism underlying resistance to specific anticancer therapies. In this study, we elucidated the interplay between metabolism and protein alterations, which significantly drive comprehensive drug resistance. We verified that, in addition to IDH, SDH deficiency represents a strong candidate molecular subtype in AML. Elevated succinate levels caused by SDH deficiency positively correlated with reduced AML PDCs' drug sensitivity across drugs classes, indicating the potential of SDH deficiency and succinate as important diagnostic and therapeutic markers in the clinical management of AML.

One of the characteristics of metabolites is their ability to enable cancer cells to respond rapidly to external stress, but the mechanism is unclear. The regulatory function of succinate in modulating protein homeostasis through activating UBC12 phosphorylation is surprising, which is independent and even earlier than transcription activation. UBC12 functions as the more important one of two E2 enzymes in neddylation³², but the mechanism of its activity regulation is limited. Intriguingly, our findings demonstrated, for the first time, that UBC12 can be phosphorylated, and we discovered a solid link between succinate-upregulated UBC12 phosphorylation and the impairment of E2 enzyme activity and cullins neddylation. We conjecture that the rapid modulation of succinate on the stability of oncoproteins through p-UBC12/cullin axis provides a primitive defense for AML cells in response to anticancer therapies. These findings also highlight p-UBC12 as an attractive target for overcoming drug resistance in tumor cells. Although the function of SDH deficiency in inhibiting cullin activity has been reported³³, our work first reveals the molecular mechanism of SDH deficiency inhibiting cullin neddylation and the resulting resistant phenotype. Besides of the upregulated proteins, we also found that succinate can downregulate some proteins, probably



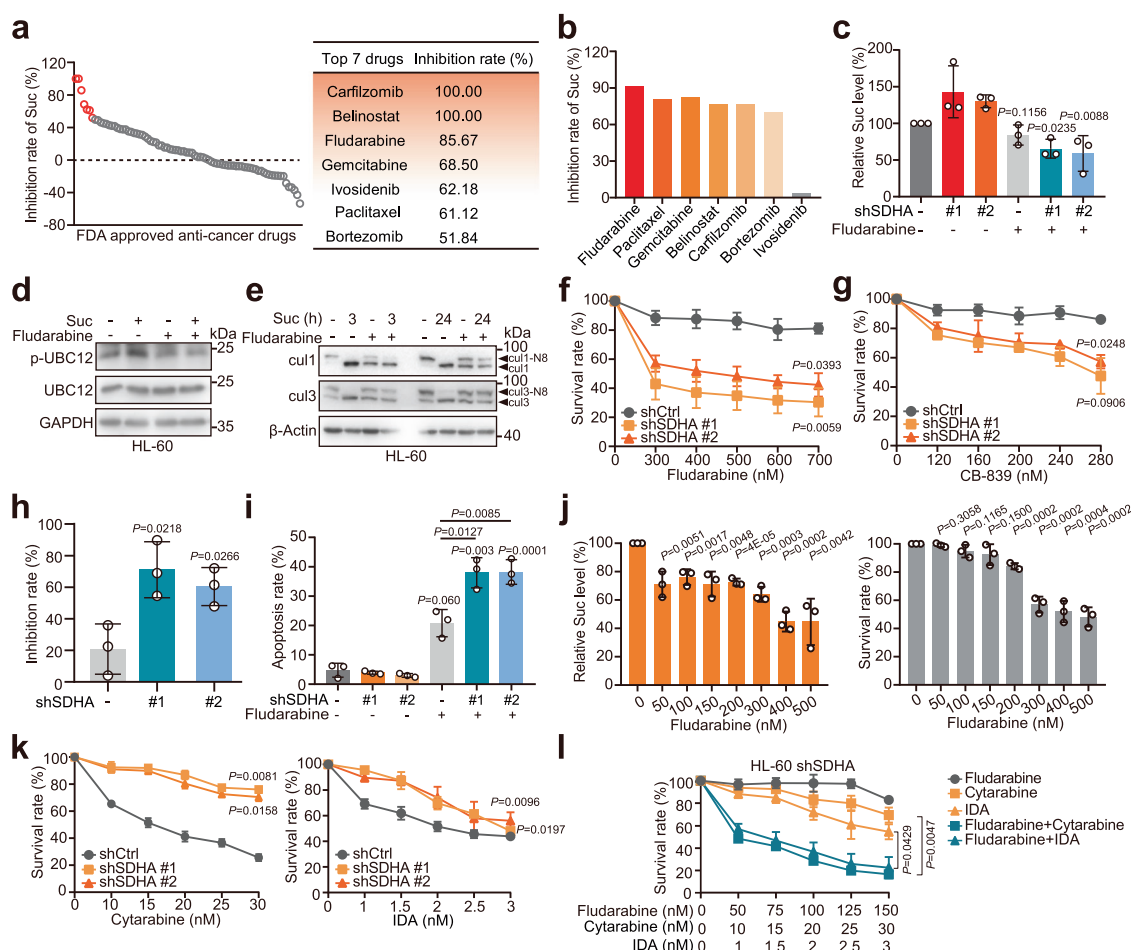
through upregulating E3 ligase and downregulating DUBs. There are some classic tumor suppressors among these downregulated proteins, like CUX1 and SETD2, which may also play a role in inducing resistance in AML and warrant further in-depth study.

The relationship between CRLs and cancers is diverse, exhibiting both cancer-promoting and anticancer effects^{34–36}. The anticancer effect of E1 enzyme inhibitor MLN4924 exhibits one aspect of this

relationship. We consider that the degree of dependence on CRLs by different tumors, as well as the activation levels of various CRL substrates in different tumors, may influence the role of CRLs in cancer. In AML, we are more inclined to consider that CRL inhibition may exert a cancer-promoting effect based on our data. This is further validated under the tumor-promotion effect of low concentrations of MLN4924 in AML cells, while the tumor-suppressing effect of high

Fig. 5 | Phosphorylation of UBC12 impairs cullins neddylation through disrupting UBC12/UBE1C interaction. **a, b**, 293 T was transfected with UBC12^{WT} and its different mutant types at S6, and their interactions with UBE1C (**a**) and DCN1 (**b**) were detected. **c** Detection of UBC12/UBE1C interaction in 293 T cells after transfected with UBE1C, followed by treatment with 100 nM TPA and 25 nM calyculin A. **d** Detection of UBC12/UBE1C interaction in 293 T cells after transfected with UBC12, followed by treatment with 200 nM sotrastaurin for 24 h. The samples derive from the same experiment but different gels for p-T/S and another for α -HA were processed in parallel. **e, f**, Detection of the transferring ability of NEDD8 from E1 enzyme. Recombinant UBE1C, NAE1 and NEDD8 proteins were incubation with

recombinant UBC12^{WT}, UBC12^{S6A}, UBC12^{S6D} or UBC12^{S6E} proteins at 2.5–15 min (**e**) and for 25–400 nM UBC12 (**f**). The samples derive from the same experiment but different gels for UBC12 and another for NEDD8 were processed in parallel. **g, h** Detection of cullin neddylation in PC9 cells after transfected with UBC12^{WT} and its different mutant types at S6 (**g**), or transfected with UBC12 and PKC α , followed by treatment with 25 nM calyculin A for 1.5 h (**h**). The samples derive from the same experiment but different gels for cul1, another for cul3 and another for cul4 were processed in parallel. The different gels for p-UBC12 and UBC12 in Fig. 5h were processed in the same way. Source data are provided as a Source Data file.



experiment but different gels for cul1 and another for cul3 were processed in parallel. **f–g** shCtrl and shSDHA HL-60 cells were treated with fludarabine (**f**) and CB-839 (**g**) for three days respectively. **h** shCtrl and shSDHA HL-60 cells were seeded in soft agar, followed by treatment with 200 nM fludarabine. After two weeks, the clones were stained and counted. **i**, shCtrl and shSDHA HL-60 cells were treated with 500 nM fludarabine for three days, and the apoptosis rates were detected. **j** Detection of intracellular succinate levels (left) and cell viability (right) of HL-60 shSDHA cells after treated by a series of concentrations of fludarabine for three days. **k–l** Cytarabine, IDA or fludarabine were treated individually or in combination to indicated cells for three days. IDA: idarubicin HCl. **c, f–l** Three independent experiments were performed. Data are presented as mean \pm SD ($n = 3$); The significance analysis were conducted by two-tailed Student's *t*-test or one-way ANOVA for Fig. 6c, **f–l**. Source data are provided as a Source Data file.

concentrations of MLN4924 may be partly due to non-cullin NEDDylation substrates, which requires further investigation. Therefore, it is necessary to discuss the role of CRLs in specific cancers.

Fludarabine is a widely used chemotherapy in hematological malignancies treatments^{37,38}. Here, we found that SDH-deficient AML PDC and PDX exhibited heightened sensitivity to fludarabine. This

increased vulnerability could be attributed to the greater dependence of SDH-deficient AML cells on elevated succinate levels. We consider that the reduction of succinate levels plays an important role in the anticancer function of fludarabine, especially at low concentrations. Although low concentrations of fludarabine may not inhibit tumor cells, they can enhance the sensitivity of SDH-deficient AML cells to

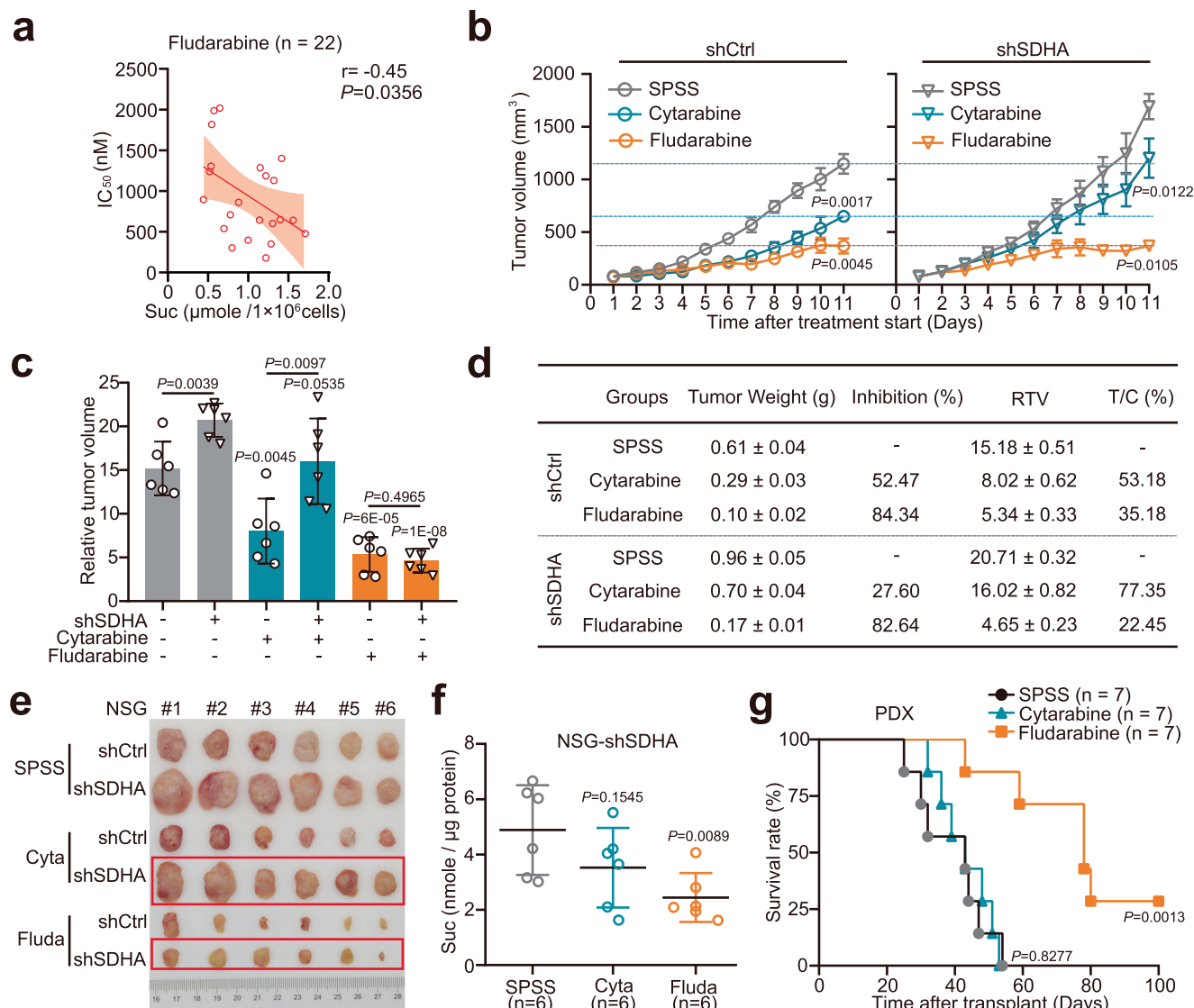


Fig. 7 | Fludarabine specifically inhibits SDH-deficient AML in both primary samples and in vivo models. a Correlation analysis between IC₅₀ of fludarabine on primary AML samples and the succinate levels of these samples. Pearson correlation coefficient r was calculated by GraphPad Prism. Data are presented as mean ± 95% confidence bands. The significance analysis was conducted by simple linear regression. **b–f** The effect of fludarabine and cytarabine on the tumor burden of shCtrl group and shSDHA group NSG mice. **(b)** Tumor growth of the xenograft models. **(c)** Relative tumor volumes of the xenograft models. **d** Effects of fludarabine and cytarabine on shCtrl group and shSDHA group tumor size and tumor

weight at pre-dose and post-dose. RTV, relative tumor volume; T/C (%) = $RTV_{\text{Treatment}}/RTV_{\text{control}} \times 100$. Data are represented as mean ± SE ($n = 6$); **(e)** Images of tumors in each treatment group. **f** The succinate levels in shSDHA group tumor tissues. The significance analysis was conducted by two-tailed paired Student's t -test for **(b)** and unpaired Student's t -test for **(c, d, f)**. **g** The survival time of AML PDX with high succinate levels treated by fludarabine (40 mg/kg) or cytarabine (60 mg/kg) by intraperitoneal injection every other day. The significance analysis was conducted by Log-rank test. Source data are provided as a Source Data file.

other anticancer drugs by reducing succinate levels. These findings provide a possibility of overcoming drug resistance in malignancies through disturbing the metabolic collapse of succinate, and highlight the broader clinical implications for fludarabine. The mechanism by which fludarabine reduces succinate levels still requires further study.

Overall, we identify SDH deficiency as a molecular subtype associated with drug resistance in AML, and dissect the regulation of oncoprotein homeostasis by succinate as a rapid and comprehensive self-protection mechanism that facilitates AML cells to resist anticancer therapies.

Methods

Ethical statement

Our research complies with all relevant ethical regulations. The use of the primary AML samples and information for researches purposes

was approved by the Institutional Research Ethics Committee of the Children's Hospital of Zhejiang University (Hangzhou, China). All mouse studies are approved by the Center for Drug Safety Evaluation and Research of ZJU.

Cells and cell culture

The HL-60 and NB4 cell lines were gifted from Dr. Lingtao Wu (University of Southern California, CA, USA). The COS-7 and PC9 cell lines were purchased from the Shanghai Institute of Biochemistry and Cell Biology (Shanghai, China). The 293 T and 293FT cell lines were purchased from Invitrogen (Grand Island, NY, USA). Primary AML blasts and primary non-AML blasts were partially extracted from the bone marrow of child patients (the Children's Hospital of Zhejiang University, Hangzhou, China) using Ficoll-Paque PREMIUM (Cytiva), and the adult primary AML and primary non-AML samples used were from

those previously reported by us³⁴. Both adult and pediatric samples were used for all the experiments. The non-AML samples used in this study were from patients who underwent bone marrow examinations due to clinical indications but were ultimately not diagnosed with AML. Both primary AML samples and primary non-AML samples included both sexes. No sex or gender analysis was carried out and the sex or gender of participants was determined based on self-report. The median age at diagnosis of AML patients was 10 years old, with ages ranging from 1 to 82 years old. The median age of non-AML donors was 18 years old, with ages ranging from 7 to 80 years old. The detailed information of these primary samples was provided in the Supplementary table 6. All primary AML blasts and primary non-AML blasts are from patients who signed informed consent and obtained participant compensation. For pediatric patients, consent from their guardians were obtained.

The HL-60, NB4 and PC9 cell lines were cultured in RPMI 1640 medium. The 293 T, 293FT and COS-7 cell lines were cultured in Dulbecco's modified Eagle's medium (DMEM). Primary AML blasts and primary non-AML blasts were cultured in IMDM medium supplemented with recombinant human IL-6 (5 ng/mL; R&D Systems), recombinant human IL-3 (10 ng/mL; R&D Systems), recombinant human SCF (50 ng/mL; R&D Systems), hydrocortisone (10 mmol/L; Sigma Aldrich, St.Louis, MO, USA), L-glutamine (2 mmol/L), 20% fetal bovine serum (Gibco BRL) and 1% penicillin/streptomycin. All of the above mediums were supplemented with 10% fetal bovine serum (Gibco BRL) and 1% penicillin/streptomycin. All cell lines were cultured in a humidified atmosphere containing 5% CO₂ and at 37 °C.

Primary blasts extraction

Primary blasts were isolated using Ficoll density gradient centrifugation. First, add 6 ml of Ficoll to a centrifuge tube, then dilute the bone marrow sample with PBS to a total of 6 ml. Mix well, and slowly layer the sample onto the Ficoll. Centrifuge the sample at 1500 rpm for 30 min at 4 °C to separate plasma and mononuclear cells. Carefully aspirate the plasma and mononuclear cells. Transfer the mononuclear cells to a new centrifuge tube and add 10 ml of PBS. Centrifuge at 1600 rpm for 5 min, discard the supernatant, and proceed with red blood cell lysis to obtain the primary blasts. For primary AML blasts, perform CD45 detection on the mononuclear cells using flow cytometry. If the percentage of primary AML blasts is greater than 80%, use them directly; if it is less than 80%, isolate the primary AML blasts through flow sorting before use.

Plasmids, reagents and antibodies

The shRNA oligonucleotides targeting SDHA were cloned into the PLKO.1 vector. The target sequences of SDHA shRNA are: #1-GATTGCTGATGGAAGCATAA and #2-TCGCTATTGCACCTTATAT, which were synthesized by TSINGKE Biological Technology. Human UBC12, UBE1C, PKC α , PKC β I and PKC β II were amplified from the 293 T cDNA library and subsequently subcloned into a pCDNA3.0 plasmid. UBC12 mutants (S6A, S6D and S6E) were produced by site-directed mutagenesis. PKC α CAT and PKC α DN were produced from PKC α plasmid. PKC β I CAT and PKC β II CAT were separately produced from PKC β I and PKC β II plasmid.

The anti-cancer drugs library was purchased from Selleck Chemicals. Fludarabine, cytarabine, cladribine, CB-839 and all PKC inhibitors were purchased from Selleck Chemicals. TPA and calyculin A were purchased from Cell Signaling Technology. Antibodies against SDHA (ab14714), UBE1C (ab124728), DCNA (ab181233), NEDD8 (ab81264), cullin 1 (ab75817) and WEE1 (ab307515) were purchased from Abcam. Antibodies against cullin 3 (#2759) was purchased from Cell Signaling Technology. Antibodies against UBC12 (SC-390064) was purchased from Santa Cruz Biotechnology. Antibodies against HA (db2603), GAPDH (db106) and β -actin (db10001) were purchased from

Diagbio. The anti-Flag antibody (HOA012FL01) was purchased from HuiOu Biotechnology. FITC anti-human CD45 (Cat#555482) and PE anti-mouse CD45 (Cat#553081) were purchased from BD Pharmingen.

Succinate determination

The succinate levels of plasma, cells and tumor tissues were detected by the Succinate Colorimetric Assay kit (Sigma-Aldrich, MAK184). The time points for succinate measurement: 1) Detection of succinate levels in primary AML patient samples: Upon receipt of primary AML samples, serum samples and mononuclear cell samples are obtained through Ficoll separation on the same day, and succinate levels in serum and cells are promptly detected. 2) Detection of succinate levels in leukemia orthotopic xenograft model: After detecting the onset of disease in mice using the CD45 marker, peripheral blood is collected from mice before euthanasia, and bone marrow cells are obtained and succinate levels are detected on the same day in both peripheral blood and bone marrow cells from both control and model mice. 3) Detection of succinate levels in SDHA knockdown cells: SDHA is knocked down in HL-60 cells using lentiviral infection, followed by two rounds of puromycin selection to establish stable SDHA knockdown cell lines, which are then sampled and tested.

Immunoprecipitation

Cells were lysed in 1% NP40 lysis buffer, containing 0.1 mM Na₃VO₄, 1 mM PMSF, and 5 mg/ml leupeptin for 30 min on ice, and then centrifuged at 13200×g for 30 min at 4 °C. The supernatants were collected and incubated with HA-tagged or Flag-tagged beads for 4 h at 4 °C. After that, the beads were washed for five times with the above 1% NP40 buffer. The beads were then boiled and separated by SDS-PAGE.

Recombinant proteins purification

Plasmids containing GST-UBC12, GST-UBC12^{S6A}, GST-UBC12^{S6D}, GST-UBC12^{S6E}, GST-UBE1C, GST-NAE1 or GST-NEDD8 were transformed into *Escherichia coli* BL21 (DE3). Isopropyl b-D-thiogalactoside (IPTG) was added in the buffer (137 mmol/L NaCl, 2.7 mmol/L KCl, 1.76 mmol/L KH₂PO₄ and 10 mmol/L Na₂HPO₄·12H₂O, pH = 7.4) to induced the expression of these proteins in bacteria. After that, the bacteria were lysed by the High-pressure Bacteria Breaker (Union Biotech), and these GST-fusion proteins was purified by the GST affinity column (GE healthcare). Next, these GST-fusion proteins were dialyzed overnight, and the GST tag was cut by the thrombin enzyme and separated by GST resin. Finally, these proteins were concentrated and quantified.

Lentivirus production and transduction

Virus production, concentration and transduction were performed as described previously³⁹.

Quantitative proteomics analysis

HL-60 cells were treated with 6 mM succinate for 3 h or 24 h and then harvested. Label-free quantitative proteomics was actualized and analyzed by PTM BIO. Three independent experiments were conducted.

RNA sequencing

HL-60 cells were treated with 6 mM succinate for 3 h or 24 h and then harvested. RNA sequencing was actualized and analyzed by Shanghai Biotechnology Corporation. Three independent experiments were conducted.

In vitro PKC-induced phosphorylation assay

The reaction buffer of in vitro PKC-induced phosphorylation assay includes 6 μ L dilution buffer (40 mM MOPS, pH 7.2; 2 mM DTT; 2 mM CaCl₂), 5 μ L PKC lipid activator and 5 μ L ATP mixture (75 mM CaCl₂;

500 μ M ATP). 2 μ g recombinant UBC12^{WT} protein or UBC12^{S6A} protein was mixed with 20 ng recombinant PKC α protein and then incubated in the reaction buffer in for 30 min at 30 °C. After that, 10 μ L loading buffer was used to terminate this reaction.

Western blotting

Western blotting was performed as described previously (Chen et al.). For detection of UBC12-NEDD8, the non-reducing system was employed as follows: 1) Lysis buffer: 50 mM MES, 150 mM NaCl, 0.2% NP40. 2) SDS-PAGE: ① 3.5x Bis-Tris gel buffer: Weigh 13.08 g Bis-Tris, dissolve in double-distilled water, adjust pH to 6.5–6.8 with concentrated HCl, and then make up to 50 mL with double-distilled water; ② 32% Acrylamide-Bis gel buffer: Weigh 15 g acrylamide and 1 g bis-acrylamide, dissolve in double-distilled water, and make up to 50 mL with double-distilled water; ③ 5x Bis-Tris Running buffer: Weigh 26.16 g MOPS, 15.14 g Tris, 0.93 g sodium EDTA, and 2.5 g SDS, dissolve in double-distilled water, and make up to 500 mL; ④ 20x Bis-Tris Trans buffer: Weigh 10.2 g Bicine, 13.1 g Bis-Tris, 0.75 g sodium EDTA, and 23.3 mg Chlorobutanol, dissolve in double-distilled water, and make up to 125 mL.

Soft agar formation assay

2 mL of 0.5% soft agar was added in the wells of the 6-well plates. After the agar mixture solidified, cells that was mixed in 0.3 % soft agar were plated on it. Then, the cells were cultured in the cell culture incubator at 37 °C for 10–14 days until the colonies grew to the appropriate size. Finally, nitroterazolium blue chloride (NBT) was used to stain the cells in the soft agar and Image J was used to count the quantities of colonies.

Animal studies

For the xenograft experiment, 1×10^7 HL-60 shCtrl cells or shSDHA (#1 and #2) cells were injected subcutaneously into female NOD-SCID IL-2receptor gamma null (NSG) mice (Shanghai Model Organisms). When the tumors reached a volume from 50 to 100 mm³, the tumor volumes were measured and recorded every day until the experimental endpoint. For studying the effects of fludarabine, 1×10^7 HL-60 shCtrl cells or shSDHA #2 cells were injected subcutaneously into NSG mice. When the tumors reached a volume from 50 to 100 mm³, the mice were treated with fludarabine (60 mg/kg; i.p.) or cytarabine (60 mg/kg; i.p.). The tumor volumes and the weights of mice were recorded every day until the experimental endpoint. The humane endpoint for animals set by our ethics committee is when the weight of a single tumor exceeds 10% of the animal's body weight, or the average diameter of a tumor in adult mice exceeds 20 mm. In this study, the maximal tumor burden was not exceeded.

For generating the AML patient-derived xenograft (PDX) model, 2×10^7 primary AML cells were injected into NSG mice (Shanghai Model Organisms) via the tail vein. The mice were treated with fludarabine (60 mg/kg; i.p.) or cytarabine (60 mg/kg; i.p.) every other day at the first week after injection. 7 patients with AML provided the samples, and 3 PDX models were generated from each patient's sample, which were then randomly divided into the SPSS, fludarabine, and cytarabine groups. The detailed information of these primary samples was provided in the Supplementary table 7. The weights and survival times of these mice were recorded. At the time of the mice's recent death, the bone marrow cells were extracted and the proportion of human CD45-positive and mouse CD45-negative (hCD45⁺mCD45⁻) cells was detected by the flow cytometry. Leukemia engraftment was considered successful when more than 1% of human hCD45⁺mCD45⁻ cells were detected in the bone marrow. The humane endpoint was established based on disease progression, along with animal weight, body condition, clinical signs, and appearance, in accordance with our ethics committee policy. No animal exceeded the humane endpoint.

All mouse studies were approved by the Center for Drug Safety Evaluation and Research of ZJU. Female NOD-SCID IL-2 receptor gamma null (NSG) mice were obtained from Shanghai Model Organisms. The mice were housed in individually ventilated cages (IVC) and were provided with sterilized food, water, and bedding. The environmental conditions for the mice were maintained at temperatures between 21 and 26 °C and humidity levels ranging from 50% to 70%.

Quantification and statistical analysis

Drug sensitivity analysis. The gene expression values in different tumor tissues and normal tissues were respectively from TCGA and GTEx, where the median expression data were downloaded from [GEPIA](https://c.sanger.ac.uk), and the expression data of each sample were downloaded from [UCSC](https://c.sanger.ac.uk). The information of gene mutations in different tumor cell lines was referred from Cell Model Passports (<https://c.sanger.ac.uk>). Genes expression values in different tumor cell lines and the Z scores of over 300 kinds of approved drugs on these cell lines were from [cancerrx-gene](https://www.cancerrxgene.org/) (<https://www.cancerrxgene.org/>).

Statistical analysis and Reproducibility

Statistical analyses were performed by GraphPad Prism 8.0.1. Two-tailed unpaired Student's t tests were employed for the comparisons between two different groups. One-way ANOVA analyzes were employed for the comparisons between three or more groups. Log-rank (Mantel-Cox) test was employed for the comparison of survival curves between two different groups. Results in vitro are expressed as mean \pm SD and results in vivo are expressed as mean \pm SEM for control and comparative groups. *P* values \leq 0.05 represented significant. Statistical testing is derived from at least three independent experiments. All western blot experiments were repeated three times independently with similar results. The investigators were blinded to group allocation during data collection and analysis.

Reporting summary

Further information on research design is available in the Nature Portfolio Reporting Summary linked to this article.

Data availability

RNA-seq data newly generated in this study have been deposited in the GEO repository at NCBI under accession codes [GSE247623](https://www.ncbi.nlm.nih.gov/geo/query/acc.cgi). Proteomics data newly generated in this study have been deposited in ProteomeXchange under accession codes [PXD047175](https://www.ncbi.nlm.nih.gov/geo/query/acc.cgi). The previous published data about the K562 transcriptome and the single-cell RNA-seq data used in this study are available in the GEO database under accession code [GSE131823](https://www.ncbi.nlm.nih.gov/geo/query/acc.cgi) [<https://www.ncbi.nlm.nih.gov/geo/query/acc.cgi>] and [GSE146590](https://www.ncbi.nlm.nih.gov/geo/query/acc.cgi) [<https://www.ncbi.nlm.nih.gov/geo/query/acc.cgi>], respectively. Source data are provided with this paper. All the other data which support the findings of this study are available with in the article, supplementary information and source data. Source data are provided with this paper.

References

- Winer, E. S. & Stone, R. M. Novel therapy in acute myeloid leukemia (AML): moving toward targeted approaches. *Therapeutic Adv. Hematol.* **10**, 2040620719860645 (2019).
- Šimoni, K. et al. Different mechanisms of drug resistance to hypomethylating agents in the treatment of myelodysplastic syndromes and acute myeloid leukemia. *Drug resistance updates : reviews and commentaries in antimicrobial and anticancer chemotherapy* **61**, 100805 (2022).
- Khawaja, A. et al. Acute myeloid leukaemia. *Nat. Rev. Dis. Prim.* **2**, 16010 (2016).
- Stine, Z. E., Schug, Z. T., Salvino, J. M. & Dang, C. V. Targeting cancer metabolism in the era of precision oncology. *Nat. Rev. Drug Discov.* **21**, 141–162 (2022).

5. van Gastel, N. et al. Induction of a timed metabolic collapse to overcome cancer chemoresistance. *Cell Metab.* **32**, 391–403.e396 (2020).
6. Eniafe, J. & Jiang, S. The functional roles of TCA cycle metabolites in cancer. *Oncogene* **40**, 3351–3363 (2021).
7. Kaelin, W. G. Jr. & McKnight, S. L. Influence of metabolism on epigenetics and disease. *Cell* **153**, 56–69 (2013).
8. Raimundo, N., Baysal, B. E. & Shadel, G. S. Revisiting the TCA cycle: signaling to tumor formation. *Trends Mol. Med.* **17**, 641–649 (2011).
9. Stuaní, L. et al. Mitochondrial metabolism supports resistance to IDH mutant inhibitors in acute myeloid leukemia. *The Journal of experimental medicine* **218**, <https://doi.org/10.1084/jem.20200924> (2021).
10. Dang, L., Yen, K. & Attar, E. C. IDH mutations in cancer and progress toward development of targeted therapeutics. *Ann. Oncol.: J. Eur. Soc. Med. Oncol.* **27**, 599–608 (2016).
11. Amar, L. et al. Succinate dehydrogenase B gene mutations predict survival in patients with malignant pheochromocytomas or paragangliomas. *J. Clin. Endocrinol. Metab.* **92**, 3822–3828 (2007).
12. Pasini, B. & Stratakis, C. A. SDH mutations in tumorigenesis and inherited endocrine tumours: lesson from the pheochromocytoma-paraganglioma syndromes. *J. Intern. Med.* **266**, 19–42 (2009).
13. Miettinen, M. et al. Immunohistochemical loss of succinate dehydrogenase subunit A (SDHA) in gastrointestinal stromal tumors (GISTs) signals SDHA germline mutation. *Am. J. surgical Pathol.* **37**, 234–240 (2013).
14. Wu, J. Y. et al. Cancer-Derived Succinate Promotes Macrophage Polarization and Cancer Metastasis via Succinate Receptor. *Mol. cell* **77**, 213–227.e215 (2020).
15. Goncalves, J. et al. Loss of SDHB promotes dysregulated iron homeostasis, oxidative stress, and sensitivity to ascorbate. *Cancer Res.* **81**, 3480–3494 (2021).
16. Velasco-Hernandez, T., Hyrenius-Wittsten, A., Rehn, M., Bryder, D. & Cammenga, J. HIF-1 α can act as a tumor suppressor gene in murine acute myeloid leukemia. *Blood* **124**, 3597–3607 (2014).
17. Lawson, H. et al. The selective prolyl hydroxylase inhibitor IOX5 stabilizes HIF-1 α and compromises development and progression of acute myeloid leukemia. *Nat. cancer*, <https://doi.org/10.1038/s43018-024-00761-w> (2024).
18. Lu, G., Wang, L., Zhou, J., Liu, W. & Shen, H. M. A destiny for degradation: interplay between cullin-RING E3 ligases and autophagy. *Trends cell Biol.* **31**, 432–444 (2021).
19. Lee, J. M., Hammarén, H. M., Savitski, M. M. & Baek, S. H. Control of protein stability by post-translational modifications. *Nat. Commun.* **14**, 201 (2023).
20. Huang, S. & Millar, A. H. Succinate dehydrogenase: the complex roles of a simple enzyme. *Curr. Opin. plant Biol.* **16**, 344–349 (2013).
21. Tseng, P. L. et al. Decreased succinate dehydrogenase B in human hepatocellular carcinoma accelerates tumor malignancy by inducing the Warburg effect. *Sci. Rep.* **8**, 3081 (2018).
22. Li, J. et al. SDHC-related deficiency of SDH complex activity promotes growth and metastasis of hepatocellular carcinoma via ROS/NF κ B signaling. *Cancer Lett.* **461**, 44–55 (2019).
23. Miller, T. W. et al. ER α -dependent E2F transcription can mediate resistance to estrogen deprivation in human breast cancer. *Cancer Discov.* **1**, 338–351 (2011).
24. Li, F. et al. CHK1 inhibitor blocks phosphorylation of FAM122A and promotes replication stress. *Mol. cell* **80**, 410–422.e416 (2020).
25. Ghelli Luserna di Rorà, A., Cerchione, C., Martinelli, G. & Simonetti, G. A WEE1 family business: regulation of mitosis, cancer progression, and therapeutic target. *J. Hematol. Oncol.* **13**, 126 (2020).
26. Esposito, F., Giuffrida, R., Raciti, G., Puglisi, C. & Forte, S. WEE1 Kinase: A Potential Target to Overcome Tumor Resistance to Therapy. *Int. J. Mol. Sci.* **22**, <https://doi.org/10.3390/ijms221910689> (2021).
27. Megger, D. A., Abou-Eid, S., Zülch, B. & Sitek, B. Systematic analysis of synergistic proteome modulations in a drug combination of cisplatin and MLN4924. *Mol. omics* **14**, 450–457 (2018).
28. Larance, M., Ahmad, Y., Kirkwood, K. J., Ly, T. & Lamond, A. I. Global subcellular characterization of protein degradation using quantitative proteomics. *Mol. Cell. Proteom.: MCP* **12**, 638–650 (2013).
29. Xu, J. et al. Chloroquine treatment induces secretion of autophagy-related proteins and inclusion of Atg8-family proteins in distinct extracellular vesicle populations. *Autophagy* **18**, 2547–2560 (2022).
30. Hirano, H. & Shirakawa, J. Recent developments in phos-tag electrophoresis for the analysis of phosphoproteins in proteomics. *Expert Rev. Proteom.* **19**, 103–114 (2022).
31. Altayb, H. N. Fludarabine, a potential DNA-dependent RNA polymerase inhibitor, as a prospective drug against monkeypox virus: a computational approach. *Pharmaceuticals (Basel, Switzerland)* **15**, 1129 (2022).
32. Zheng, Y. C. et al. Targeting neddylation E2s: a novel therapeutic strategy in cancer. *J. Hematol. Oncol.* **14**, 57 (2021).
33. Yuan, T. et al. SDHA/B reduction promotes hepatocellular carcinoma by facilitating the deNEDDylation of cullin1 and stabilizing YAP/TAZ. *Hepatol. (Baltim., Md.)* **78**, 103–119 (2023).
34. Shao, X. et al. The palmitoyltransferase ZDHHC21 regulates oxidative phosphorylation to induce differentiation block and stemness in AML. *Blood* **142**, 365–381 (2023).
35. Dai, X. et al. Prostate cancer-associated SPOP mutations confer resistance to BET inhibitors through stabilization of BRD4. *Nat. Med.* **23**, 1063–1071 (2017).
36. Fan, J. et al. Clinical significance of FBXW7 loss of function in human cancers. *Mol. cancer* **21**, 87 (2022).
37. Anderson, V. R. & Perry, C. M. Fludarabine: a review of its use in non-Hodgkin's lymphoma. *Drugs* **67**, 1633–1655 (2007).
38. Moufarij, M. A., Sampath, D., Keating, M. J. & Plunkett, W. Fludarabine increases oxaliplatin cytotoxicity in normal and chronic lymphocytic leukemia lymphocytes by suppressing interstrand DNA crosslink removal. *Blood* **108**, 4187–4193 (2006).
39. Chen, Y. F. et al. Arctigenin impairs UBC12 enzyme activity and cullin neddylation to attenuate cancer cells. *Acta pharmacologica Sin.* **44**, 661–669 (2023).

Acknowledgements

This work was supported by grants from the Young Scientists Fund of the National Natural Science Foundation of China (No. 82404667); the Natural Science Fund for Distinguished Young Scholars of Zhejiang Province (No. LR23H310001); Zhejiang Provincial Natural Science Foundation (LQ24H310005) and the China Postdoctoral Science Foundation (2023M743066).

Author contributions

M.Y. and Y.C. conceived the whole study and analyzed data; Y.C. performed drug screening assay; M.X. performed co-immunoprecipitation assay and phosphorylation-related assay, as well as western blotting; Y.C. and W.Y. performed succinate level detection, cell proliferation, and clone formation assay; S.B. analyzed the sequencing data of primary AML samples and the single-cell RNA-seq data. Y.C., J.L., X.W., and J.Y. tested the drug sensitivity; Y.C., W.Y., J.L. and S.X. performed animal assay; X.X. provided the primary AML samples; X.S. J.C., Q.H., and B.Y. helped organize the paper; M.Y., Y.C., and M.X. wrote the manuscript.

Competing interests

The authors declare no competing interests.

Additional information

Supplementary information The online version contains supplementary material available at <https://doi.org/10.1038/s41467-024-53398-9>.

Correspondence and requests for materials should be addressed to Meidan Ying.

Peer review information *Nature Communications* thanks Jean-Francois Peyron, and the other, anonymous, reviewer(s) for their contribution to the peer review of this work. A peer review file is available.

Reprints and permissions information is available at <http://www.nature.com/reprints>

Publisher's note Springer Nature remains neutral with regard to jurisdictional claims in published maps and institutional affiliations.

Open Access This article is licensed under a Creative Commons Attribution-NonCommercial-NoDerivatives 4.0 International License, which permits any non-commercial use, sharing, distribution and reproduction in any medium or format, as long as you give appropriate credit to the original author(s) and the source, provide a link to the Creative Commons licence, and indicate if you modified the licensed material. You do not have permission under this licence to share adapted material derived from this article or parts of it. The images or other third party material in this article are included in the article's Creative Commons licence, unless indicated otherwise in a credit line to the material. If material is not included in the article's Creative Commons licence and your intended use is not permitted by statutory regulation or exceeds the permitted use, you will need to obtain permission directly from the copyright holder. To view a copy of this licence, visit <http://creativecommons.org/licenses/by-nc-nd/4.0/>.

© The Author(s) 2024